future transportation

MDPI

Article

Simulation of the Turning Assistant in Road Traffic Accident Reconstruction

Ferenc Ignácz [1,*], Andreas Moser [2], Gyula Kőfalvi [3], Dániel Feszty [4] and István Lakatos [1]

[1] Vehicle Maintenance and Diagnostics Department, Audi Hungaria Faculty of Automotive Engineering, Széchenyi István University, Egyetem tér 1, 9026 Győr, Hungary; lakatos@sze.hu
[2] Dr. Steffan Datentechnik Ges.m.b.H., Niederreithstraße 39, 4020 Linz, Austria; moser@dsd.at
[3] EBK-Hungary Mérnöki, Termelő, Kereskedelmi Korlátolt Felelősségű Társaság, Újvár u. 13, 1037 Budapest, Hungary; ibbkofal@t-online.hu
[4] Department of Whole Vehicle Engineering, Audi Hungaria Faculty of Automotive Engineering, Széchenyi István University, Egyetem tér 1, 9026 Győr, Hungary; feszty.daniel@sze.hu
* Correspondence: ignacz.ferenc@sze.hu

Abstract

The accurate simulative reconstruction of blind spot accidents requires innovative simulation methods. The objective of this paper is to analyze the avoidability of a specific blind spot accident and assess the impact of various parameters as if an active turning assistant had been installed in the truck. Additionally, it proposes a novel adaptation of the turning assistant system, along with an adapted simulation model tailored for drawbar trailers. The analyses presented in this paper were performed using PC-Crash accident simulation software, applying the "Active Safety" module. After performing a simulation of an accident involving a right-turning truck with a center axle trailer and a pedestrian, the avoidability of the accident was examined by simulating the scenario as if the truck involved in the accident had been equipped with an active turning assistant system. Subsequently, a parameter analysis was conducted to analyze the effect of changes in the active turning assistant's parameters and changes in the pedestrian's direction of entry on the avoidability of the accident. In doing so, we determined the parameters for the worst-case (collision) and the best-case (no collision) scenarios. Finally, an adaptation and further development of the active turning assistant, along with a corresponding simulation method for drawbar trailers, are proposed.

Keywords: PC-Crash; simulation; ADAS; road traffic accident; heavy goods vehicle; VRU

Check for updates

Academic Editor: Jian Ma

Received: 27 October 2025
Revised: 9 December 2025
Accepted: 22 December 2025
Published: 8 January 2026

Correction Statement: This article has been republished with a minor change. The change does not affect the scientific content of the article and further details are available within the backmatter of the website version of this article.

Copyright: © 2026 by the authors. Licensee MDPI, Basel, Switzerland. This article is an open access article distributed under the terms and conditions of the Creative Commons Attribution (CC BY) license.

1. Introduction

1.1. Importance and Primary Motivations of the Research Topic

There are about 1.2 million traffic fatalities worldwide every year [1]. Reducing road fatalities is therefore necessary in all parts of the world. For example, the European Union aims to reduce the number of fatalities to nearly zero by 2050 [2]. These goals can only be achieved through a combination of comprehensive road safety measures, targeted research, and innovative technical solutions. Any contribution that helps reduce fatalities and injuries in road traffic accidents is therefore of high importance.

The area around the vehicle that is not visible or only partially visible through its exterior mirrors or windows is referred to as a blind spot. Blind spot accidents occur when a vulnerable road user (VRU) is present or moving within this area and is subsequently struck by the vehicle due to the driver's lack of visibility. The risk caused by blind spots

can be substantially reduced through the use of Advanced Driver Assistance Systems (ADASs) [3]. In the case of right-turning situations, the turning assistant—also known as cornering assistant or blind spot assistant—is particularly important.

With the ever-widening spread of driver assistance systems and (partially) self-driving vehicles, vehicle accident reconstruction experts are increasingly faced with the challenges of reconstructing road traffic accidents involving vehicles with such systems. Accurate and reliable reconstruction of accidents of this type requires special knowledge of the technical characteristics and peculiarities of vehicles equipped with these systems. In addition, the continuous development of modern special accident simulation software suitable for the reconstruction of such accidents is essential.

Based on the above, the following 3 key motivations can be formulated for our research topic:

1. Research into the sensor parameters of active turning assistant systems, the pedestrian's direction of travel, and the critical cases determined by changes in these factors is crucial. This work can directly contribute to the optimization of future active turning assistant systems, thereby indirectly improving road safety.
2. More accurate accident simulation methods—for example, regarding the drawbar trailers discussed in this research—can help reconstruct real-life road accidents more accurately, allowing more precise conclusions to be drawn regarding accident causation and supporting the development of appropriate safety measures.
3. In line with the proposal made in our current research, this includes a proposal that active turning assistant systems should also be adapted for drawbar trailers.

1.2. Literature Review

Numerous turning assistant systems are available on the market, including retrofit options for commercial vehicles. ADAC tested 5 such systems and recommended, among other things, that these systems be linked to an emergency braking system in the future [4]. This essentially means that the vehicle will automatically apply emergency braking in an emergency situation, where hitting the VRU cannot be prevented by any other means. According to the systematic classification of driver assistance systems, the active turning assistant can be defined as an active-safety function [5], since it actively tries to avoid an accident in a near-accident situation (by braking) or, in a worse case, attempts to reduce the negative consequences of an impending accident.

Mercedes' Active Sideguard Assist (ASGA) system is capable of initiating an active braking maneuver and braking the vehicle to a standstill in critical situations when the driver fails to respond to the warning signals introduced in the first and second warning stages [6].

One of the simulation methods that can be used to investigate blind spot accidents is the use of three-dimensional visibility field models which are attached to the vehicle model and move with it. This method is based on 2D visibility fields that the driver must be able to see in external vehicle mirrors—interpreted at the level of the road surface—as specified in the regulations [7]. The aforementioned method allows for the three-dimensional analysis of the visibility of a VRU positioned or moving near the vehicle. It is important to emphasize that this method is limited to analyzing the visibility ranges defined by regulations and does not take into account the fact that the actual visible area in the mirrors usually exceeds the minimum requirements specified in the standards [7]. In addition, this method cannot be used to analyze the active turning assistant as a driving assistant system and its influence during a specific accident.

The integration of driver assistant systems' modules and functions into accident simulation programs began decades ago, such as ESP [8]. The increasingly widespread active safety systems in modern cars can have a significant influence on vehicle dynamics

during an accident. Moser and Steffan conducted a simulation in which a user-configurable modular system consisting of blocks was implemented, which is suitable for simulating active systems. In their study, they also presented the simulation models of the Brake Assistant (BA) and Adaptive Cruise Control (ACC) systems, as well as test results with a real vehicle equipped with a Brake Assistant. Based on the test results, the simplified simulation model of the Emergency Brake Assistant correlated well with the real behavior of the system in the vehicle. An important conclusion of the study is that since obtaining the parameters and detailed information of the real system can be difficult, the results of real driving tests can be used for this [9].

Niewöhner, on the other hand, pointed out in his work that the understanding of the functionality of Advanced Driver Assistance Systems is often incomplete, and it is sometimes difficult to understand why a particular system reacts in a certain way. One such system is the Advanced Emergency Braking (AEB), where a number of factors influence whether or not the system brakes at a given point [10].

Paula et al. conducted an international, questionnaire-based research with experts involved in accident analysis. Based on this evaluation, they determined that a significant number of road accidents involving the ADAS cannot be conclusively reconstructed, since considerable and important technical information is missing, such as the influence of the ADAS on vehicle dynamics in the pre-collision phase. Ultimately, the implementation of the so-called Forensic Event Data Recorder (FEDR) was proposed, which would satisfy all needs from the perspective of accident experts [11].

Ritter et al. analyzed 10 real-life accidents and their avoidability, where each accident involved a right-turning heavy goods vehicle (HGV) and a cyclist as a VRU. The simulations were performed using PC-Crash, one of the leading simulation software used for traffic accident reconstruction, which is also capable of parameterizing and modeling the turning assistant, among other driver assistant systems. During the simulation analyses, the parameters of the turning assistant were changed, and their effect on the avoidability of the accident was examined. According to the results, all 10 examined accidents could have been avoided—or in some cases, the consequences of the accident could have been reduced—had the turning assistant been installed [12].

König et al. conducted tests of various systems and accident situations in order to understand the operation and limitations of the blind spot assistance system. Among other factors, the lateral distance between the VRU and the heavy commercial vehicle was found to heavily influence the reliability of the assistance system [13].

New methods for the simulation of ADASs have been continuously developed to date [14–18], and if we look at the development trends of the past period, they represent enormous research potential for the coming decades.

When reviewing modern accident analysis and investigation methods, LLM (Large Language Model) based systems should definitely be mentioned. Such systems can be used, among other things, to extract important accident-related information (e.g., vehicle data) from accident documentation in a short time [19]. The most important research in terms of our research topic can be considered promising, among other things, in the field of improving traffic safety [20].

1.3. Research Gaps

The literature review above has shown that, although numerous simulations have been conducted for ADASs and the active turning assistant, none of them analyzed the influence of the turning assistant parameters (e.g., the length of the area covered by the sensor and the braking deceleration) and the VRU direction of entry on the possibility of avoiding an accident in detail and in their context.

Therefore, to fill this research gap, one of the aims of this paper is to investigate this field through a series of simulations and parameter analyses in order to determine which combinations of sensor coverage lengths, vehicle braking deceleration and pedestrian directions of entry result in the "worst-case" scenario (a collision) and the "best-case" scenario (no collision).

An additional research gap arises from the fact that no active turning assistant system has yet been developed or installed on drawbar trailers, nor has it been examined whether hitting a pedestrian during intersection turning maneuvers with such trailers could be avoided if an active turning assistant were present.

Furthermore, the active turning assistant module of the simulation software must be adapted for drawbar trailers, as the development of a simulation methodology for commercial-vehicle accidents, with specific consideration of turning assistant systems for drawbar trailers, is crucial.

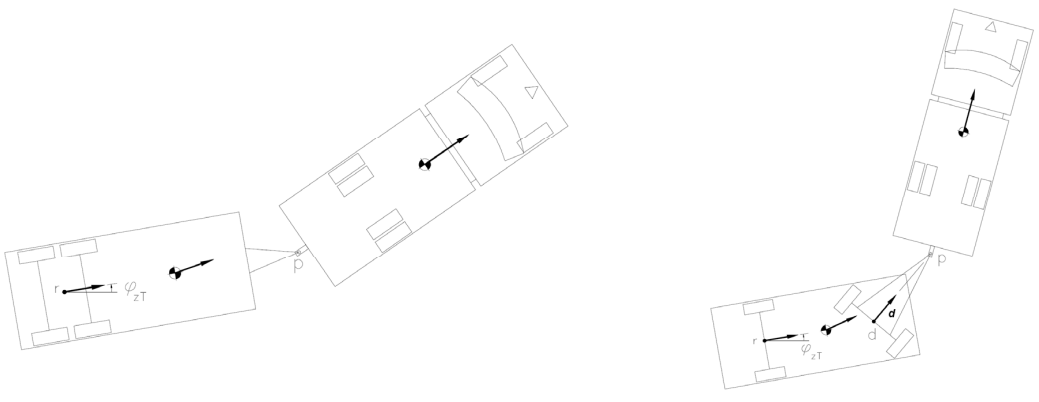
2. Methods

2.1. On PC-Crash

The simulative reconstruction of accidents with heavy commercial vehicles is significantly more complex than that of passenger cars due to their more intricate mechanics and special operating characteristics, which in turn calls for a different approach and methods [7,21]. PC-Crash 15.1 was used in this research, which can be used for the reconstruction and analysis of vehicle accidents and other incidents. PC-Crash is used by researchers, universities, expert offices, and the automotive industry, among others. The models in the software have been validated with numerous publications and countless crash tests over the past 20 years [8,22–27].

2.2. Trailer Simulation in PC-Crash

As we conducted our research by simulating trucks with trailers, we took advantage of the software's capability to simulate accidents involving multi-body vehicle combinations, which form a complex mechanical system. It is possible to simulate several types of articulated vehicles consisting of towing vehicles and trailers commonly used in practice [28]. Among these, unsteered-axle combinations (Figure 1a) and steered front axle (Figure 1b) (drawbar) trailers are particularly relevant to our research. The special feature of the trailer simulation model implemented in PC-Crash is its ability to account for the additional external forces acting between the towing vehicle (truck) and the towed vehicle (trailer) during collisions and driving [25].



(**a**) (**b**)

Figure 1. Simulation models of unsteered (**a**) and steered (**b**) trailers attached to the truck in PC-Crash [27].

The post-impact motion of the pedestrian was simulated using a multi-body system (MBS), the theoretical background and application areas of which are described in the relevant literature [27].

2.3. Approaches to Simulating ADASs in PC-Crash: Focus on the Turning Assistant

PC-Crash includes pre-defined active safety systems [27], which enable simulation systems such as ABS, ESP, ACC, TCS, EBA and TA (Turning Assistant), which is particularly relevant to this study. The modular, block-based system allows the user to build and flexibly configure the active safety systems according to the vehicle they are simulating. The active safety systems of vehicles can be assembled using parameterizable and programmable blocks, e.g., sensors, algorithms and actuators [9]. The main modules of the system are the distance sensor, steering check and braking module (Figure 2).

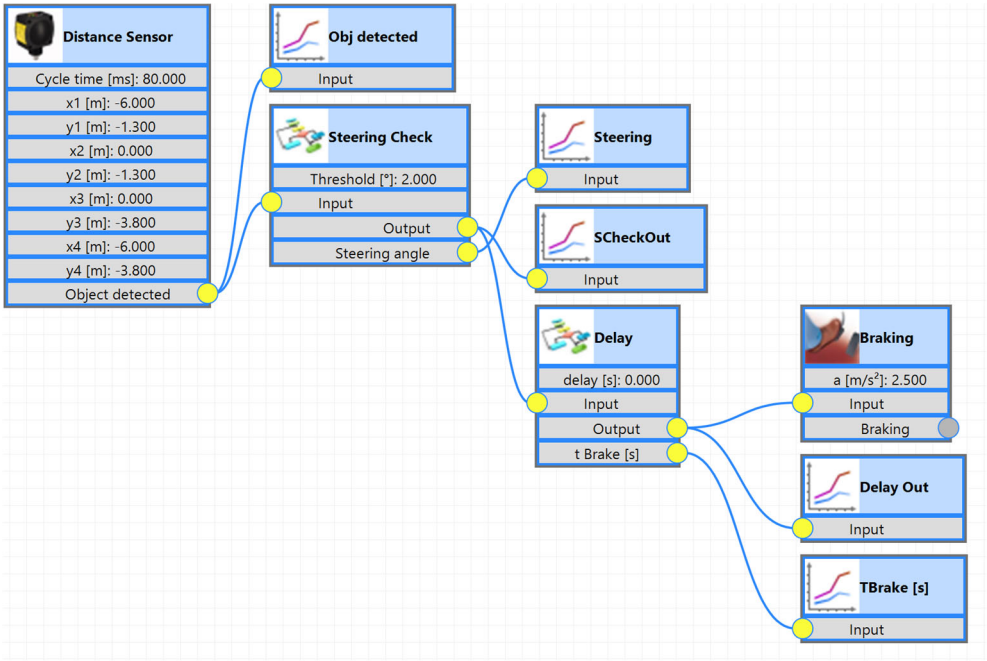


Figure 2. System architecture of the (active) turning assistant in PC-Crash with default settings.

Real active turning assistant systems, which use sensors to monitor VRUs in blind spots next to the vehicle, typically operate in several stages. If a VRU enters the blind spot but does not yet pose an immediate risk (first stage), the driver is typically warned with an optical signal. If the situation escalates and becomes dangerous (second stage), the optical signal is supplemented with an acoustic signal. In the third stage, the system automatically starts a braking process and brakes the vehicle to a standstill [6]. In our simulations, only the influence of the size of the sensor area relevant to the active braking process was examined, as this parameter plays a crucial role in avoiding accidents when the driver fails to react. The earlier stages of the active turning assistant that provide visual and acoustic warnings prior to automatic emergency braking were not included in the scope of this research. Therefore, only the third stage of the system was simulated during the avoidability tests. This essentially means that the drivers' potential reaction and their impact in the simulation were not examined (stage 1–2), but the vehicle's automatic braking was considered in the event of no driver reaction.

The truck simulation model collects data using the active safety module in the following way: A 2D surface with geometric data defined in the module represents the sensor area relevant for emergency braking. Automatic emergency braking occurs if the pedestrian

simulation model overlaps with the relevant sensor area of the truck or trailer during the driving simulation.

According to the default software settings, the active turning assistant system initiates immediate braking when a pedestrian enters the area covered by sensors. Therefore, latency is equal to zero in avoidability simulations. No intervention delay was taken into account in the case of the active turning assistant, as the effect of this parameter was not part of the present investigation.

Our analysis is not based on legal requirements or type-specific active turning assistance parameters. Instead, we relied on the default settings and parameters defined in PC-Crash, which we then varied to analyze their influence during the simulations.

2.4. Representation of Simulation Results and Search for a Mathematical Relationship Approximating the Results

To present the results of all avoidability simulations, we created a 3D surface in MATLAB® R2025b. This surface illustrates how the safety distance varies as a function of two parameters: the length of the sensor area and the pedestrian's direction.

Based on the data and results discussed in Section 3.4, we aimed to identify a mathematical relationship that describes the results of the avoidability simulations. For this purpose, we applied the "Curve Fitter" application of MATLAB® R2025b, using a fitting procedure:

1. After testing several functions to approximate the simulation results, the following two-variable quadratic polynomial (type: poly22) was selected, since it can be used to describe the surface showing the safety distances in the relevant range with an accuracy of 5%:

$$f(x,y) = p00 + p10 \cdot x + p01 \cdot y + p20 \cdot x^2 + p11 \cdot x \cdot y + p02 \cdot y^2$$

2. The coefficients of this equation were determined using the "Curve Fitter" application of MATLAB® R2025b.

Although degrees (°) are used throughout this paper for ease of understanding pedestrian entry directions, all fitting procedures, fitting-related calculations, and a parameter in the equation express the entry direction in radians [-].

2.5. Sequence of Research Procedures and Other Factors Relevant to the Simulations

First, a road traffic accident involving a right-turning truck with a center axle trailer and a pedestrian was reconstructed using simulations. Next, the avoidability of the accident was investigated under the assumption that the truck had been equipped with an active turning assistant. A parameter analysis was then conducted to examine how changes in the active turning assistant's parameters and the pedestrian's direction of entry affected the potential to avoid the accident. Finally, an adapted version of the active turning assistant system and an adapted simulation model for drawbar trailers are proposed.

The intersection, where the specific accident and its avoidability were analyzed by simulation, was modeled on a flat surface. There was no significant slope or elevation at the site, nor was there any level difference that would have influenced the simulation results. The drawing of the intersection was prepared using the drawing module in PC-Crash based on an on-site survey of the geometric data.

The movement process of the vehicle combination following the collision was simulated using the kinetics forward simulation method, which models the vehicle's forward movement in time, taking into account external forces (e.g., tire forces). The road surface was dry at the time of the accident, which will be taken into account during the computer mathematical simulation of the accident mechanism with a friction factor of $\mu = 0.8$. The mentioned friction factor refers to the friction factor between the road's surface and the

tires of the vehicle. The pre-collision movement of both the vehicle combination and the pedestrian was simulated using a reverse kinematics calculation method.

Since elderly individuals are exposed to a significantly higher risk of death in traffic accidents [29], there is significant room for improvement in their safety. This is why we focused on them in this study.

3. Results and Discussion

The purpose of this section is to perform a simulation analysis on the avoidability of a blind spot accident. The lack of an active turning assistant system in the truck contributed to a pedestrian being hit. As our first step, we simulatively reconstructed the accident, forming the basis for the avoidability study. Then, we analyzed whether the pedestrian would have been hit by the right-turning truck had it been equipped with an active turning assistant system. During our analysis, we determined the best and worst-case scenarios by changing and then analyzing the influence of the active turning assistant's parameters and the pedestrian's direction of entry. Finally, in the last subsection, we propose the necessity of installing active turning assistants on drawbar trailers, as well as the further development of an adapted simulation model.

3.1. Accident Situation and Initial Data

In the Section 3.2 we present the simulation of an accident between an HGV combination and a pedestrian as a VRU, and then we examine the avoidability of the accident under the assumption that an active turning assistant has been installed in the truck of the vehicle combination. According to the available data, the accident occurred as follows: during a right-hand turn at the intersection, the vehicle combination hit a pedestrian—who was crossing the road adjacent to the designated pedestrian crossing, moving in a direction nearly parallel to it—with the front right of the vehicle. Unfortunately, the pedestrian suffered fatal injuries. There were no permanent deformations on the truck. The truck driver reversed the truck a short distance after the accident. The accident reconstruction diagram was created using the drawing module in PC-Crash (Figure 3).

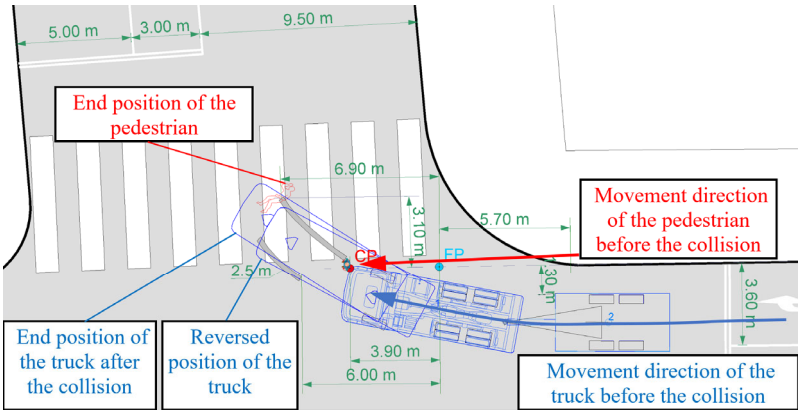


Figure 3. Reconstruction diagram of the accident scene.

The vehicle combination consists of a three-axle truck and a two-axle (center axle) trailer. The total length of the vehicle combination is $l_{v\text{-}c}$ = 14.3 m. The axle configuration of the truck is 6 × 4, and its maximum permissible total weight (gross vehicle weight) is m = 26 t. The vehicle combination was traveling without cargo at the time of the accident. Detailed geometrical and mass data of the truck and trailer of the vehicle combination are presented in Table 1.

Table 1. Geometric and mass data of the truck and trailer in the accident simulation.

Description	Name/Value	
	Truck	**Towed Trailer**
Manufacturer	MAN	Kögel
Type	TGA 26.430 6 × 4 BB	ZK 18
Length	7.730 m	4.970 m
Width	2.500 m	2.500 m
Height	3.511 m	2.600 m
Front overhang	1.525 m	2.000 m
Total weight	11,900 kg	4622 kg
Wheelbase $(A - B_1)/(C_1 - C_2)$	3.200 m	1.300 m
Wheelbase $(B_1 - B_2)$	1.400 m	-

The pedestrian involved in the accident was an 80-year-old female, h = 1.67 m tall.

The collision of the pedestrian and her movement process following the collision were simulated with a multi-body model.

3.2. Simulation of the Accident

According to the reconstructed related positions, the truck had already initiated a right turn before the moment of the collision, while the pedestrian was moving next to the pedestrian crossing, almost parallel to it (Figure 4).

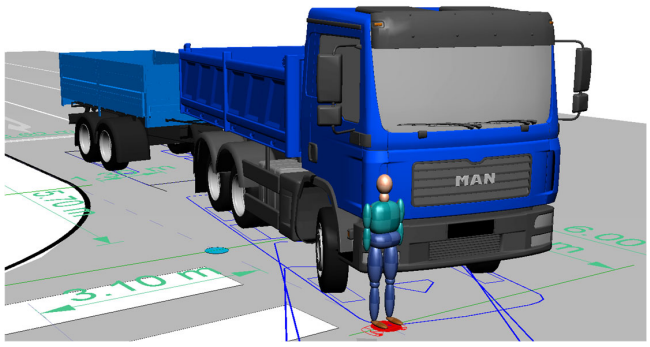


Figure 4. Reconstructed collision position of the pedestrian and truck in PC-Crash.

The movement process of the participants after the collision is shown in time steps of t = 0.5 s in Figure 5. With the simulation, we also determined the swept path of the vehicle combination, which represents the area delimited by orange lines.

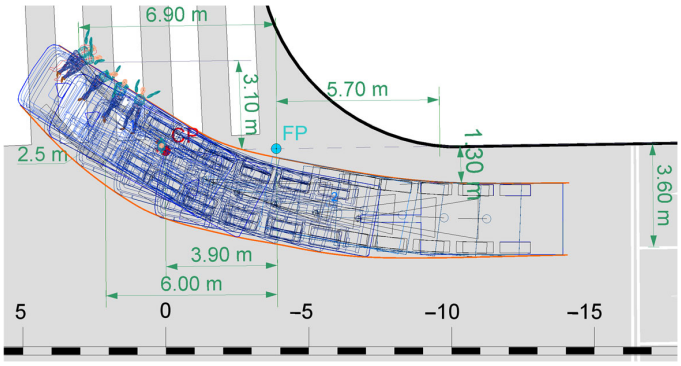


Figure 5. Post-crash moving process of the participants in time steps of t = 0.5 s.

The pedestrian's movement distance after being hit is s_{ped} = 4.2 m. According to simulation results, the pedestrian could have fallen onto the road at t = 0.5 s after being hit and then could have rebounded slightly off the road. After that, from t = 1.0 s until reaching her end position, i.e., until t = 2.4 s, the pedestrian drifted on the road in front of the right front wheel of the truck (Figure 6).

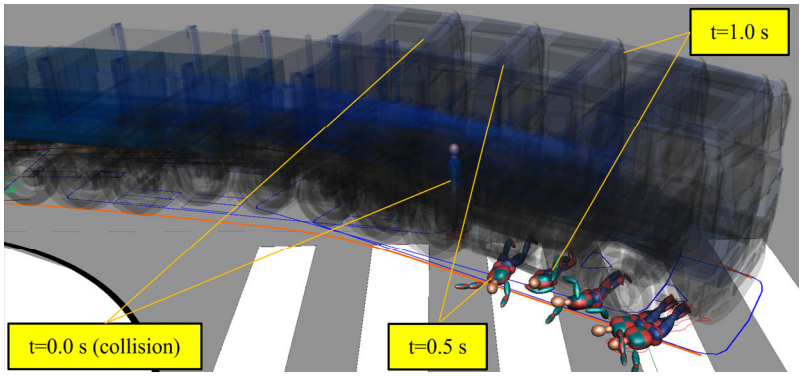


Figure 6. Post-collision moving process of the participants in time steps of t = 0.5 s.

The pedestrian's end position was in front of the right wheel of the truck's 'A' axle, partially trapped beneath it (Figure 7).



Figure 7. End position of the pedestrian and the truck.

The distance-time graph depicting the post-collision process of the truck is shown in Figure 8.

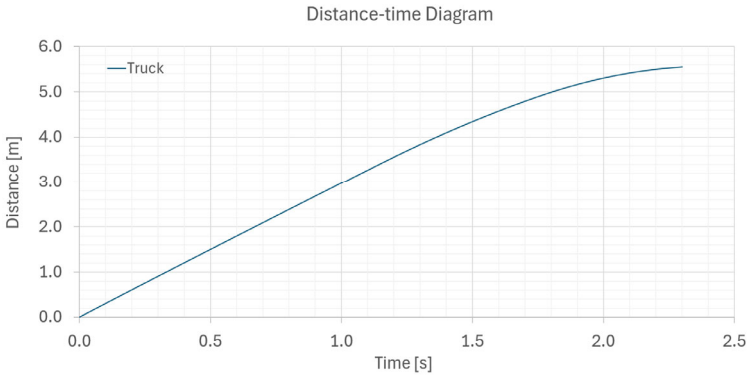


Figure 8. Distance-time diagram of the truck.

Based on the results of the simulation, the collision velocities and directions of travel at the time of the collision, as presented in Table 2, could be determined.

Table 2. Collision values.

Description	Accident Participant	Value
Collision velocity	Truck	11.1 km/h
	Pedestrian	3.6 km/h
Collision direction	Truck	165.0°
	Pedestrian	−179.3°

We performed a simulation of the accident participants' movement process prior to impact. The simulation was performed using a reverse calculation method. The vehicle combination started the turning process from the right-turning lane. In the simulation, the vehicle combination was traveling at a constant velocity of $v_{v\text{-}c}$ = 11.1 km/h, while the pedestrian was also traveling at a constant velocity of v_{ped} = 3.6 km/h towards the point of impact. Before being hit, the pedestrian was moving in the immediate vicinity of the pedestrian crossing, approximately parallel to the extended line of the edge of the road (Figure 9).

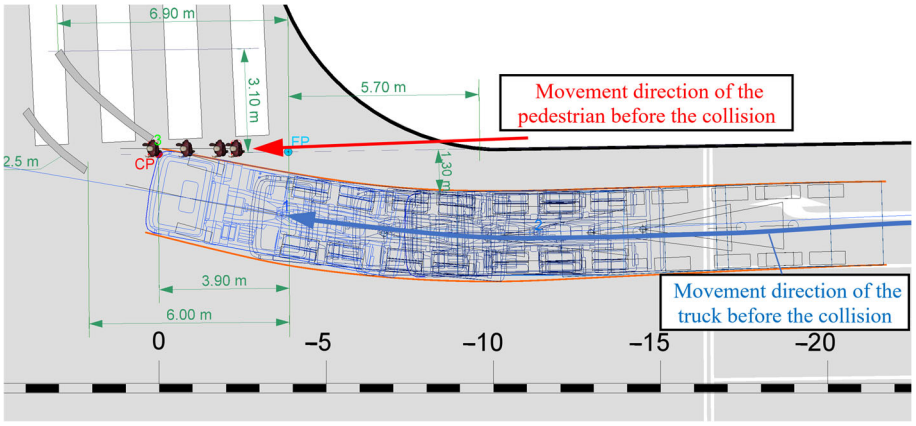


Figure 9. Pre-collision process of the participants in time steps of t = 1.0 s.

Figure 10 shows the reconstructed pre-collision positions of the vehicle combination and the pedestrian at t = 2.5 s before impact. In this situation, the pedestrian was s_{ped} = 2.5 m, and the vehicle combination was $s_{v\text{-}c}$ = 7.7 m from the point of impact. Concerning the pre-collision process, the swept path of the vehicle combination was also determined, which is marked with orange lines.

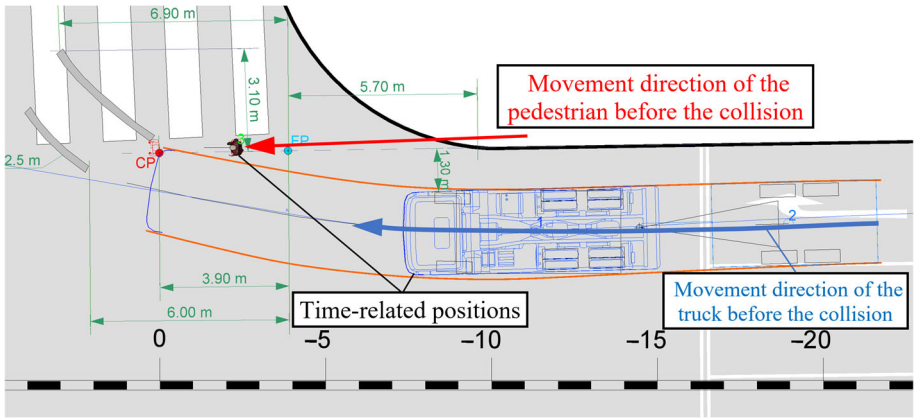


Figure 10. Position of the participants t = 2.5 s before the collision ($v_{v\text{-}c}$ = 11.1 km/h; v_{ped} = 3.6 km/h).

3.3. Simulation of Accident Avoidability Owing to the Presence of an Active Turning Assistant

In the following simulation, we examined whether the collision with the pedestrian could have been avoided if the truck had been equipped with an active turning assistant system. The active turning assistant module in PC-Crash has been assigned to the towing vehicle of the vehicle combination, i.e., the truck (Table 3).

Table 3. System settings of the active turning assistant (truck).

Description	Parameter	Value
Sensor settings	Cycle time	80 ms
	Length	9.7 m
	Width	2.5 m
Active braking settings	Delay	0.0 s
	Deceleration	$-2.5\ m/s^2$

When the active turning assistant is activated, the default deceleration value defined for the entire vehicle combination is $a_{v\text{-}c} = -2.5\ m/s^2$. The structure of the system is presented in Figure 11.

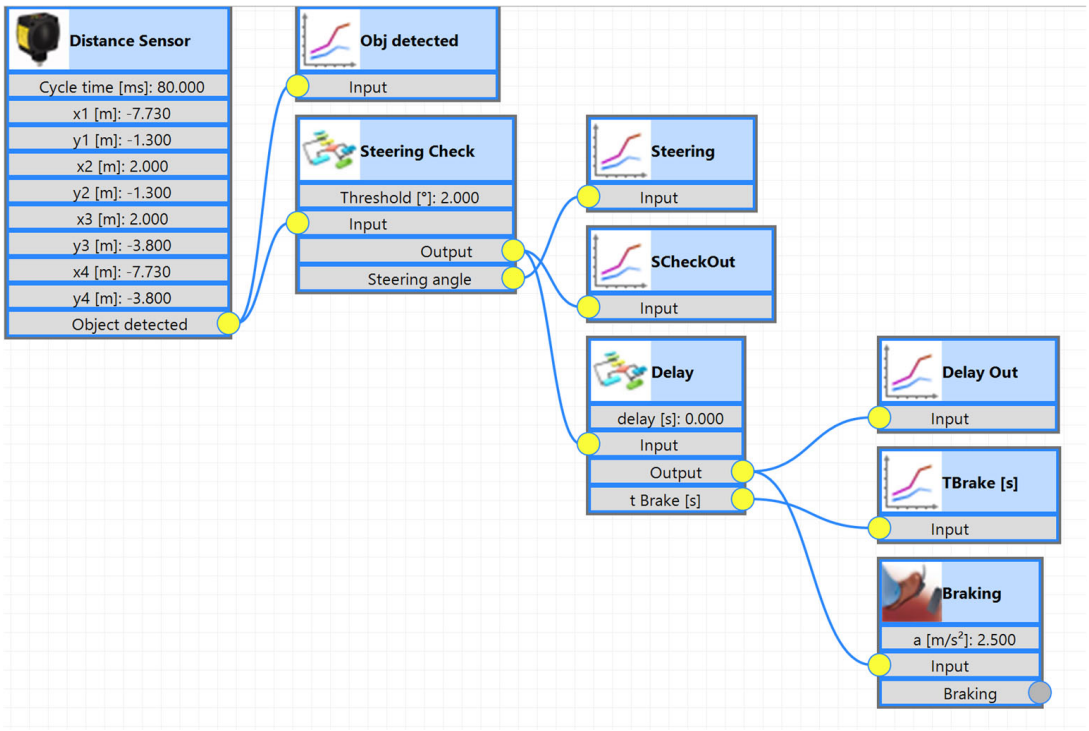


Figure 11. System model for the active turning assistant in PC-Crash.

In the default model, the sensor-detected area relevant to the active braking process extends 2.0 m forward from the front of the truck. The default settings of the active turning assistant were modified to the extent that the length of the area covered by the sensors was adjusted to the rear of the truck (Figure 12).

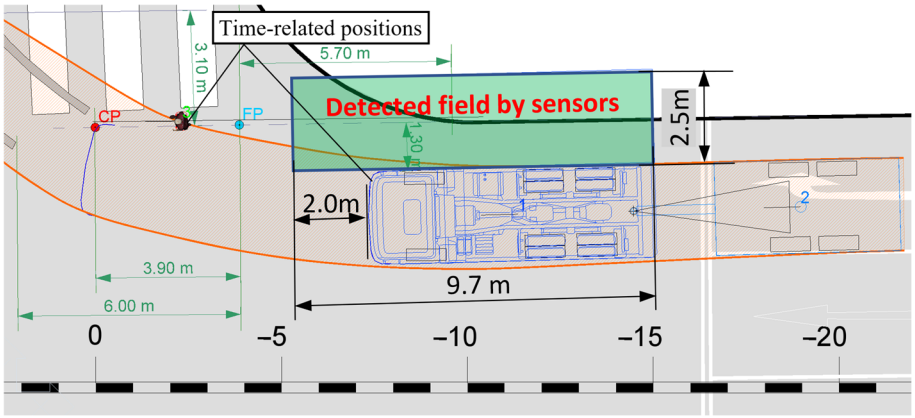


Figure 12. Position of the participants and the sensor-detected field relevant to the active braking process.

The avoidability simulation showed that if the truck had been equipped with an active turning assistant system at the time of the accident, the accident could have been avoided. According to the results of the avoidability simulation, the moment the vehicle combination braked to a standstill, the pedestrian would have been moving at a distance of s = 1.54 m in front of the truck's front end (Figure 13).

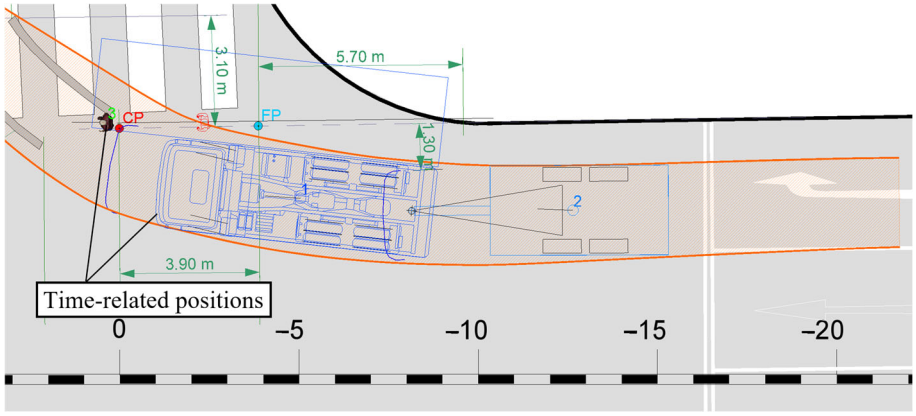


Figure 13. Avoidability simulation with the active turning assistant.

The distance-time graphs of the individual participants in the avoidability simulation are shown in Figure 14.

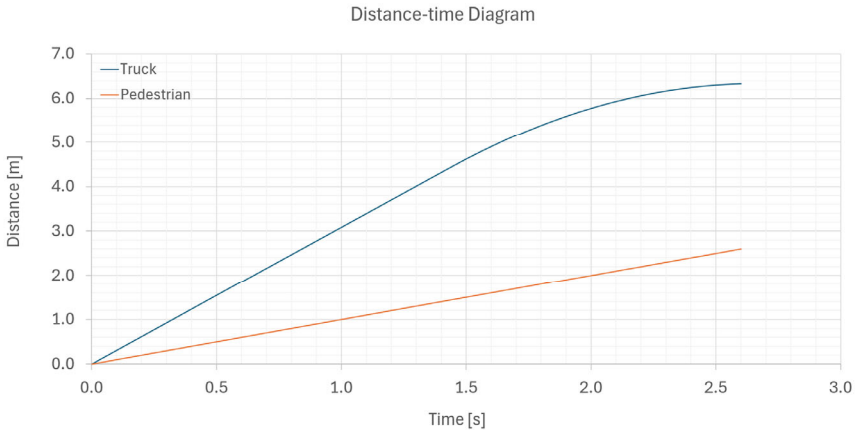


Figure 14. Distance-time diagram of the vehicle combination and the pedestrian.

3.4. Parameter Analysis with Active Turning Assistant

In this parameter analysis, we examined how the avoidability of the accident simulated in Section 3.2 would have developed if the parameters of the active turning assistant and the pedestrian's direction of entry were changed. During the parameter analysis, we performed a total of 45 simulations in series, during which the following parameters were changed:

- The length of the area covered by the active turning assistant's sensors: 9.7+/−1 m (the length of the covered area was changed at its front line).
- The deceleration of the vehicle combination during the operation of the active turning assistant occurred in the following steps: $a_{v\text{-}c}$ = −1.5 m/s^2; −2.5 m/s^2 (default); −3.5 m/s^2; −4.5 m/s^2 and −5.5 m/s^2.
- The pedestrian's direction of entry relative to the direction of travel at the time of the accident: α_{ped} = 0° (original direction), and then α_{ped} = 30° and α_{ped} = 60° (relative travel directions if the original travel direction at the time of the accident is considered 0°).

During the simulations, the velocity of the pedestrian and the vehicle combination was kept constant, using the reconstructed values in accident reconstruction ($v_{v\text{-}c}$ = 11.1 km/h; v_{ped} = 3.6 km/h). Upon the activation of the turning assistant, the velocity of the vehicle combination decreased according to the braking deceleration defined in the given simulation. No intervention delay was defined for the active turning assistant, as the effect of this parameter was not investigated. In the simulations, the vehicle combination moved according to the swept path determined in the accident reconstruction. During the evaluation of the simulation results, we investigated whether the collision occurred under the given parameters and, if so, determined the corresponding collision velocities for the vehicle combination. In cases where no collision occurred, we measured the smallest distance between the pedestrian and the front of the truck the moment the vehicle combination breaks to a standstill. A summary of the simulation results is presented in Table 4.

Table 4. Simulation results of the parameter analysis: distances between the truck and the pedestrian the moment the vehicle combination breaks to a standstill, as well as collision velocities (if available). (a) The red numbers illustrate the cases in which the pedestrian would be hit (residual distance equals zero). (b) The orange numbers illustrate cases where the critical residual distance is less than 1 m. (c) The green numbers illustrate the cases where the critical residual distance is more than 1 m. (d) The red box illustrates the worst-case scenario. (e) The green box illustrates the best-case scenario.

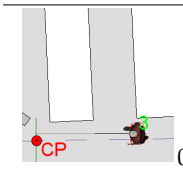
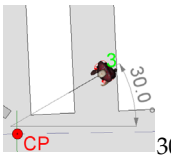
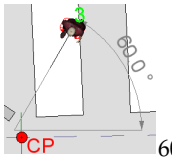
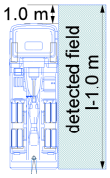
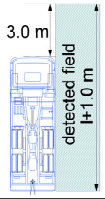
		Simulated Residual (Safety) Distances		
		Direction of pedestrian movement		
The length of the area covered by the sensors	Deceleration of the vehicle combination $a_{v\text{-}c}$ [m/s^2]	 0° (default)	 30°	 60°
	−1.5	0.00 ($v_{c\text{-}a}$ = 7.3 km/h)	0.00 ($v_{c\text{-}a$ = 7.8 km/h)	0.00 ($v_{c\text{-}a$ = 8.5 km/h)
	−2.5 (default)	0.39	0.14	0.00 ($v_{c\text{-}a$ = 6.2 km/h)
	−3.5	0.59	0.42	0.00 ($v_{c\text{-}a$ = 1.7 km/h)
	−4.5	0.69	0.58	0.25
	−5.5	0.75	0.68	0.40

Table 4. *Cont.*

		Simulated Residual (Safety) Distances		
	−1.5	1.08	0.60	0.00 ($v_{c\text{-}a}$ = 4.8 km/h)
	−2.5 (default)	1.54	1.25	0.67
	−3.5	1.75	1.58	1.14
	−4.5	1.87	1.77	1.41
	−5.5	1.89	1.81	1.55
	−1.5	2.08	1.89	0.99
	−2.5 (default)	2.55	2.62	2.04
	−3.5	2.75	2.93	2.52
	−4.5	2.87	3.10	2.79
	−5.5	2.90	3.19	2.97

According to the results of the simulations, if the length of the area covered by the sensors is reduced by 1.0 m in the first line of the area, and the deceleration value of the vehicle combination is reduced by 1.0 m/s^2 ($a_{v\text{-}c}$ =− 1.5 m/s^2), the collision with the pedestrian occurs in every range of entry angles (0°: default; 30°; 60°). Among these cases, the highest collision velocity would have occurred at a pedestrian entry angle of 60° (Figure 15). We defined this case as the worst-case scenario (shown in red frame in Table 4).

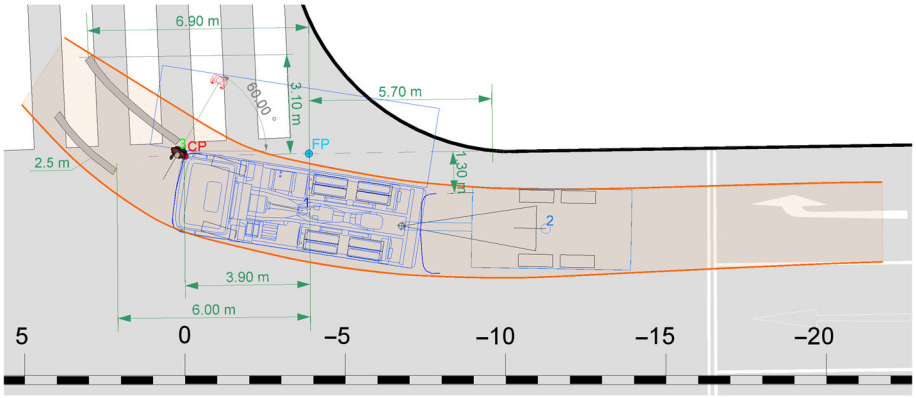


Figure 15. Worst-case scenario with collision: α_{ped} = 60°; l_{area} − 1 m; $a_{v\text{-}c}$ = −1.5 m/s^2; $v_{v\text{-}c}$ = 8.5 km/h; v_{ped} = 3.6 km/h.

In the best-case scenario without collision (in the case of an increased sensor coverage area, with increased deceleration and a pedestrian entry angle of 30°), the pedestrian would have been in motion at about s_{ped} = 3.2 m in front of the truck the moment the vehicle combination braked to a standstill (Table 4—in green frame) (Figure 16).

In the case of the default ($a_{v\text{-}c}$ = −2.5 m/s^2) and the increased ($a_{v\text{-}c}$ = −3.5 m/s^2) vehicle combination deceleration values, as well as a sensor coverage area reduced by 1.0 m, the collision would have occurred only at a pedestrian entry angle of 60°. At the other entry angles (0° and 30°), the collision could have been avoided (Figure 17). However, the moment the vehicle combination braked to a standstill, the pedestrian, who was in motion, would have been extremely close, within a distance of 1.0 m, similar to deceleration values $a_{v\text{-}c}$ = −4.5 m/s^2 and $a_{v\text{-}c}$ = −5.5 m/s^2 (shown with orange numerical values in Table 4).

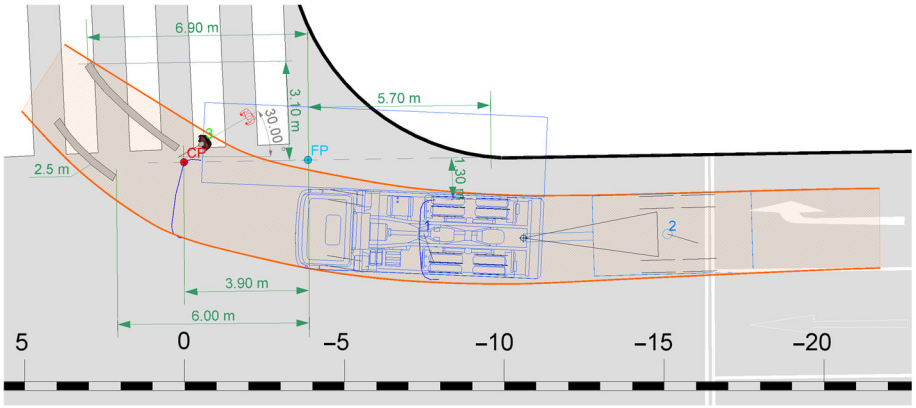


Figure 16. Best-case scenario without collision: α_{ped} = 30°; l_{area} + 1 m; $a_{v\text{-}c}$ = −5.5 m/s^2; $v_{v\text{-}c}$ = 0.0 km/h; v_{ped} = 3.6 km/h.

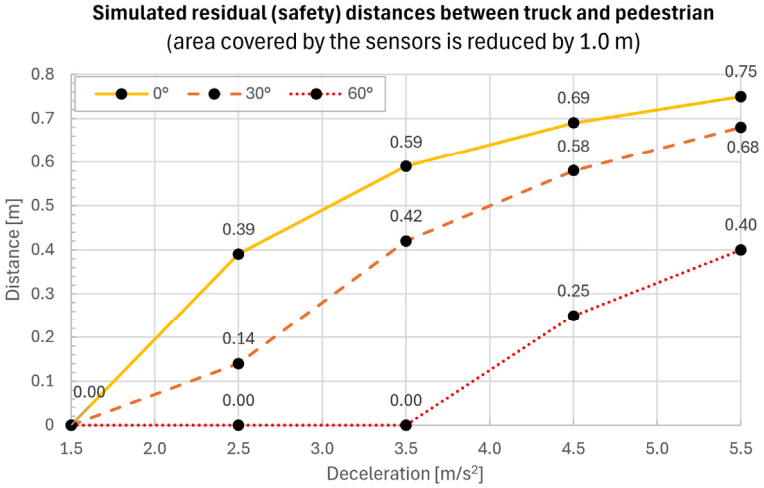


Figure 17. Results from the simulations with reduced sensor area.

Analyzing all cases where the deceleration value was $a_{v\text{-}c}$ = −4.5 m/s^2 and $a_{v\text{-}c}$ = −5.5 m/s^2, the pedestrian would not have been hit. Based on this, it can be concluded that the active turning assistant—considering the parameters and other data from the present analysis—generally enables accident avoidance in cases where the deceleration value is −4.5 m/s^2 and more intense.

Simulation results indicate that as the pedestrian's entry angle increases, the residual (safety) distance tends to decrease when the sensor coverage area is set to its default or a reduced length (Figures 17 and 18). This can essentially be explained by the geometric characteristics of the area covered by the sensor (length-width ratio), as the pedestrian entered the area covered by the sensor at a later time. As a result, the braking of the vehicle combination also begins at a later time, which results in a smaller distance between the participants at the start of the emergency braking, which ultimately leads to a smaller residual distance.

The longer the sensor coverage area, the smaller the effect of the pedestrian's movement direction on the safety distance. This is most noticeable at the upper deceleration value of $a_{v\text{-}c}$ = −5.5 m/s^2 (Figure 19).

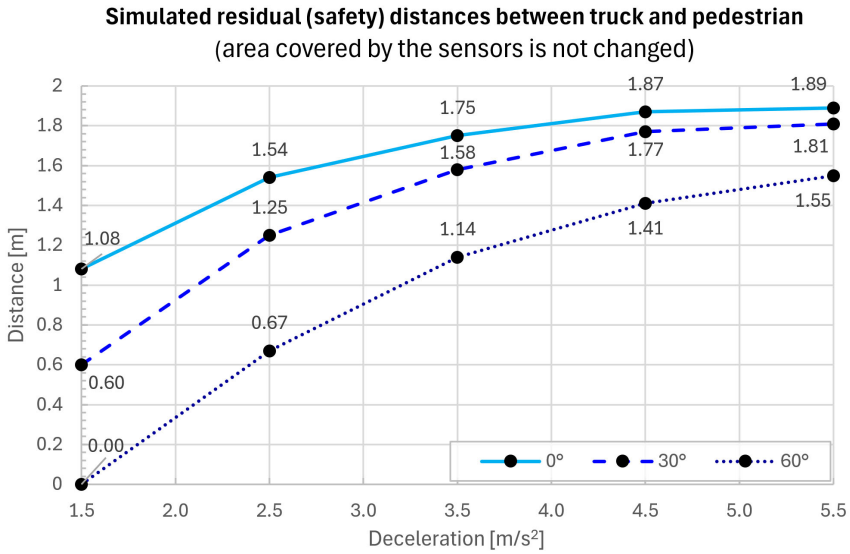


Figure 18. Results from the simulations with default sensor area.

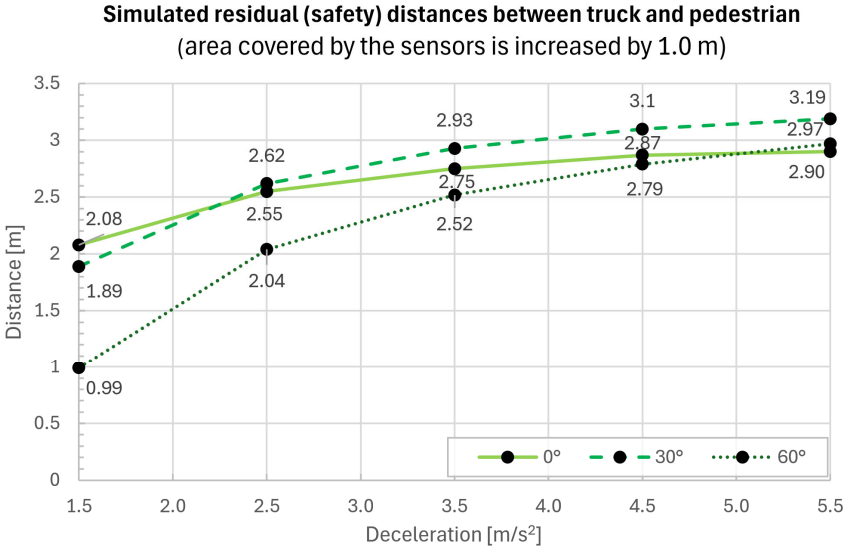


Figure 19. Results from simulations with increased sensor area.

Evaluating the simulation results for the—in absolute terms—upper deceleration value of the vehicle combination ($a_{v\text{-}c} = -5.5$ m/s^2), the length of the sensor area has a significantly greater effect on the residual safety distance than the entry direction of the pedestrian. This is especially noticeable at the 60° entry angle, where increasing the length of the sensor area by 2 m results in a 7.4-fold increase in residual distance (Figure 20).

In order to establish the mathematical equation that describes the 3D surface based on simulated results, we performed surface fitting in MATLAB® [30] and approximated the results with a polynomial surface of type poly22 (Figure 21).

Based on the simulation results, the following polynomial equation can be established for the residual (safety) distance:

$$f(x,y) = a + b{\cdot}x + c{\cdot}y + d{\cdot}x^2 + e{\cdot}x{\cdot}y + f{\cdot}y^2 \quad (1)$$

The description and values of the equation components are presented in Table 5.

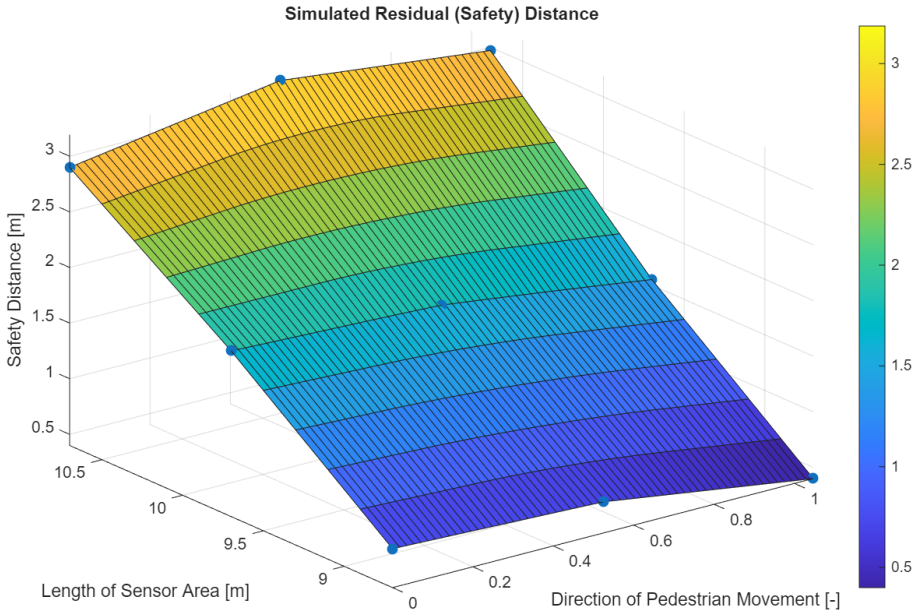


Figure 20. Simulation results for the deceleration value of $a_{v\text{-}c} = -5.5\ m/s^2$ (created by the author in MATLAB® R2025b). The blue dots illustrate the simulated residual (safety) distances.

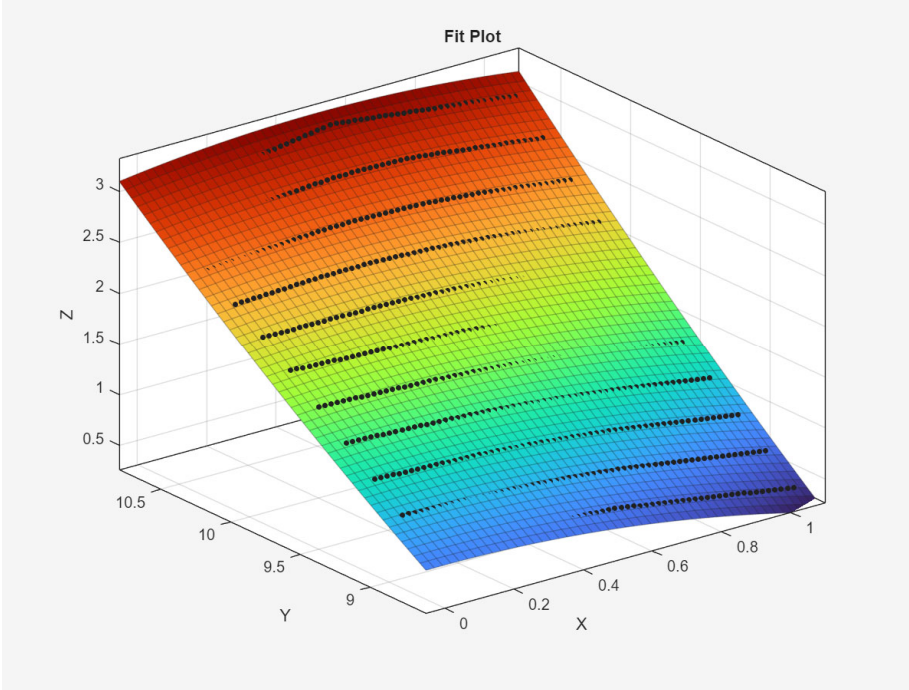


Figure 21. Surface fitting of the simulation results (created by the author in MATLAB® Curve Fitter), where X—direction of pedestrian movement [-], Y—length of sensor area [m], Z—safety distance [m]. (a) The black dots illustrate the simulated residual (safety) distances and intermediate points. (b) The colored surface illustrates the surface fitted to the simulation results.

The surface fitting results calculated with Equation (1) correlate well with the simulated values for most of the values and show less than 5% deviation (Tables 6 and 7). A larger deviation is shown only when the length of the sensor area is decreased and the pedestrian entry direction is 60°. Since the decreased length of the sensor area is undesirable due to minimal safety distance, Equation (1) is suitable for determining the safety distance in the relevant range.

Table 5. Equations content.

Designation	Value	Unit	Type	Description
x	0; 0.52; 1.05	-	variable	Entry direction of the pedestrian (radian)
y	8.7; 9.7; 10.7	m	variable	Length of the sensor area
a	−2.198	-	coefficient	-
b	−1.732	-	coefficient	-
c	−0.283	-	coefficient	-
d	−0.415	-	coefficient	-
e	0.201	-	coefficient	-
f	0.072	-	coefficient	-

Table 6. Fitting of the simulated values (calculated values with Equation (1)).

Fitting Results [m]		Entry Direction of the Pedestrian		
		0.00°	**30.00°**	**60.00°**
Length of the sensor area	8.70 m	0.78	0.67	0.34
	9.70 m	1.82	1.81	1.59
	10.70 m	3.00	3.10	2.98

Table 7. Deviation of fitting results from simulation results [%].

Deviation of Fitting Results from Simulation Results [%]		Entry Direction of the Pedestrian		
		0.00°	**30.00°**	**60.00°**
Length of the sensor area	8.70 m	3.76	−1.29	−15.66
	9.70 m	−3.88	0.27	2.32
	10.70 m	3.41	−2.75	0.27

3.5. Proposal for the Development of an Active Turning Assistant and Its Simulation Model for Drawbar Trailers

Experience in real accident scenarios has shown that a turning truck's drawbar trailer—turning in a smaller radius—can hit vulnerable road users crossing an intersection, e.g., pedestrians. This usually occurs when the driver of a heavy goods vehicle fails to detect a VRU approaching in the blind spot area or when it is obscured by other objects. Unfortunately, it is also possible that the HGV driver is inattentive and fails to detect a VRU approaching or staying close to their vehicle. To simulate this accident situation, the intersection and the towing truck presented in Section 3.1 were used as a basis. The truck's central axle trailer was replaced with a drawbar trailer (Table 8), and the pedestrian's path was modified so that it intersected with the right side of the drawbar trailer as the pedestrian crossed the crosswalk.

During the simulation, both the previously determined swept path of the vehicle combination and the previously reconstructed travel speeds were taken into account. Without an active turning assistant on the trailer, the pedestrian collides with the right side of the drawbar trailer between the trailer's axles C1 and C2 (Figure 22).

Table 8. Geometric and mass data of the truck and trailer in the simulation with drawbar trailer.

Description	Name/Value	
	Truck	**Drawbar Trailer**
Manufacturer	MAN	Schwarzmüller
Type	TGA 26.430 6 × 4 BB	-
Length	7.730 m	8.580 m
Width	2.500 m	2.550 m
Height	3.511 m	3.035 m
Front overhang	1.525 m	0.780 m
Total Weight	11,900 kg	5800 kg
Wheelbase $(A - B_1)/(C_1 - C_2)$	3.200 m	4.660 m
Wheelbase $(B_1 - B_2)$	1.400 m	1.400 m

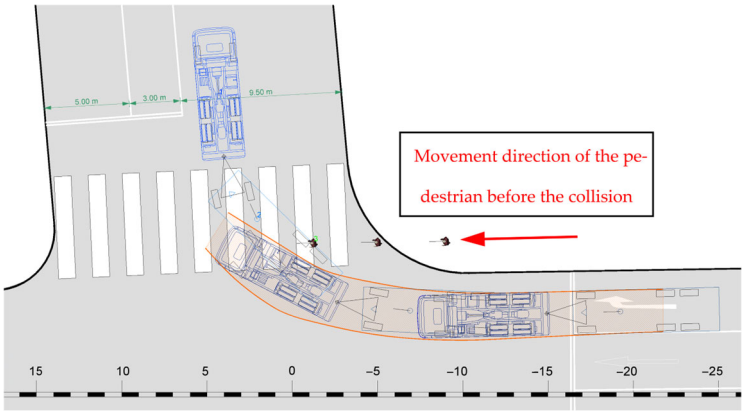


Figure 22. Accident scenario between drawbar trailer and VRU (initial velocities: $v_{v\text{-}c}$ = 11.1 km/h; v_{ped} = 3.6 km/h; time step: t = 4.0 s; collision at t = 7.8 s).

Based on the results of the simulation avoidability analysis previously performed and described in detail in Section 3.3 of this paper, it can be assumed that if drawbar trailers were also equipped with an active turning assistant system, accidents where the trailer of the turning vehicle combination hits the VRU could be prevented. To investigate this, we conducted a simulation based on the intersection and the truck presented in Section 3.1. During the model creation process, we adapted the active turning assistant simulation module to a simulation model of a three-axle drawbar trailer, connected to the truck (Figure 23).

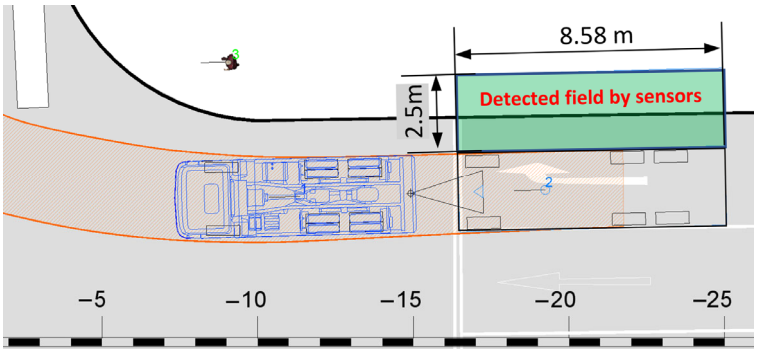


Figure 23. Simulation model adapted to a new vehicle category: drawbar trailer equipped with active turning assistant system.

Based on an analysis conducted with the adapted simulation model, we determined that if the drawbar trailer had been equipped with an active turning assistant system in the described situation, the pedestrian would not have been hit (Figure 24).

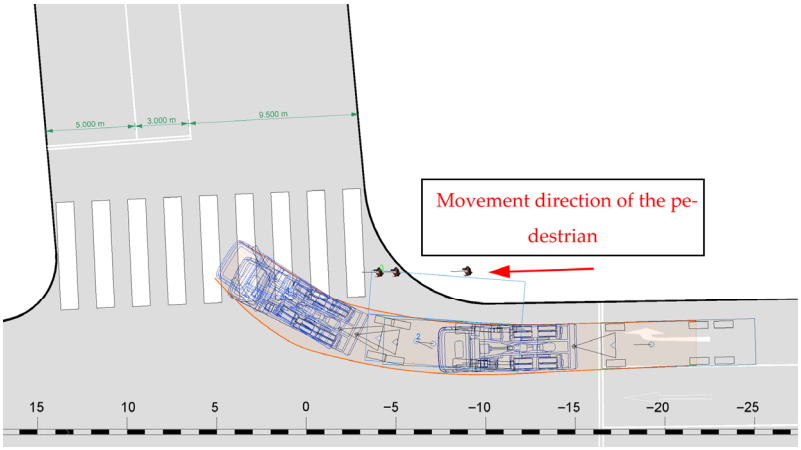


Figure 24. Avoidability simulation with the simulation model, adapted to a new vehicle category: Drawbar trailer equipped with active turning assistant system (included in PC Crash)/(initial velocities: $v_{v\text{-}c}$ = 11.1 km/h; v_{ped} = 3.6 km/h; $a_{v\text{-}c}$ = −2.5 m/s^2; time step: t = 4.0 s; standstill at t = 4.9 s).

The distance-time graphs of the individual participants in the simulations are shown in Figure 25.

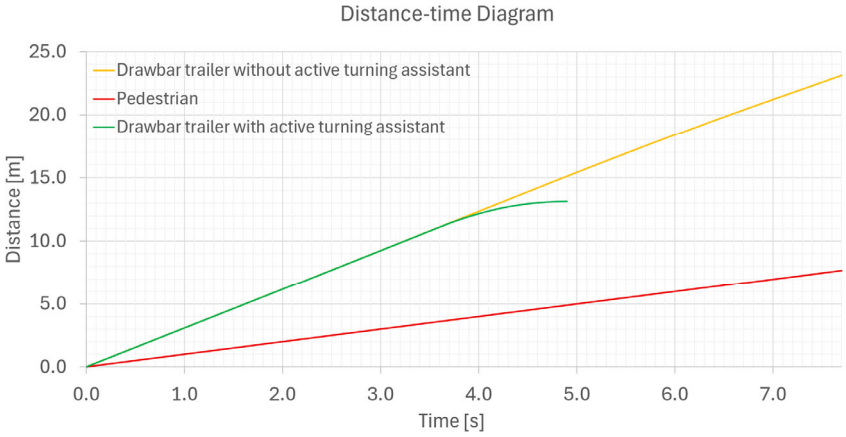


Figure 25. Distance-time diagram of the pedestrian and the drawbar trailer with and without active turning assistant.

We argue that active turning assistants should be installed not only on towing vehicles but also on drawbar trailers, in order to help save lives and prevent serious injuries caused by trailer-related accidents. However, for practical applicability, several parameters—including the area covered by the sensor(s)—need to be precisely determined. Therefore, in the next step of our research, we will conduct and publish a further parameter analysis.

This corresponding active turning assistant simulation model for drawbar trailers based on the above analysis could then be used to efficiently investigate such accidents. Drawing from the data and parameters of the active turning assistant system to be developed for drawbar trailers, we will further develop the simulation model presented here, which will also be utilized in the next phase of our research. We propose further research

and development of active turning assistant systems and its simulation model for drawbar trailers, as this system could prevent trailer collisions with VRUs.

4. Conclusions

Based on the simulation of a real accident, it was established that if the right-turning vehicle combination had been equipped with an active turning assistant at the time of the accident, the collision with the pedestrian could have been avoided. In this case, the pedestrian would have moved at a distance of s = 1.54 m from the front of the truck the moment the truck braked to a standstill.

Drawing from the simulated data of the real accident, a parameter analysis based on the results of a total of 45 simulations was conducted. These simulations served as the basis for defining the worst-case and best-case scenarios. According to the worst-case scenario, a high-velocity collision would have occurred with a reduced coverage area, low deceleration and a pedestrian entry angle of 60°. In the best-case scenario (in the case of an increased coverage area, with increased deceleration and a pedestrian entry angle of 30°), the pedestrian would not have been hit, and the pedestrian would have been in motion approximately 3.2 m in front of the truck the moment the vehicle combination braked to a standstill.

When analyzing the default ($a_{v\text{-}c} = -2.5\ m/s^2$) and increased ($a_{v\text{-}c} = -3.5\ m/s^2$) deceleration values of the vehicle combination, along with a sensor coverage area reduced by 1.0 m, the collision would have occurred only at a pedestrian entry angle of 60°. At the other entry angles (0° and 30°), the collision could have been avoided, although the remaining safety distance was minimal (<1.0 m), similar to the cases with—in absolute terms—higher deceleration values ($a_{v\text{-}c} = -4.5\ m/s^2$ and $a_{v\text{-}c} = -5.5\ m/s^2$). The pedestrian would not have been hit in cases where the deceleration value was $a_{v\text{-}c} = -4.5\ m/s^2$ and $a_{v\text{-}c} = -5.5\ m/s^2$. Accordingly, it can be concluded that the active turning assistant—taking into account the parameters and other data from the present analysis—makes it possible to avoid the accident where the deceleration value is $a = -4.5\ m/s^2$ or more intense. Based on the analysis of the simulation results, it can even be stated that an increase in the pedestrian's entry angle generally results in a decrease in the residual (safety) distance.

Simulation results indicate that as the pedestrian's entry angle increases, the residual (safety) distance tends to decrease when the sensor coverage area is set to its default or a reduced length. The longer the sensor coverage area, the smaller the impact of the pedestrian's movement direction on the safety distance. This effect is most pronounced at the higher deceleration value of the vehicle combination ($a_{v\text{-}c} = -5.5\ m/s^2$). When evaluating the simulation results for $a_{v\text{-}c} = -5.5\ m/s^2$, the sensor coverage length has a significantly greater influence on the residual safety distance than the pedestrian's entry angle.

The surface fitting results calculated with Equation (1) show good agreement with the simulation data for most values, with a deviation of less than 5%. Larger deviations occur only when the sensor coverage is reduced and the pedestrian entry direction is 60°. Since a reduced sensor coverage results in minimal safety distances and is therefore undesirable, the proposed equation is suitable for determining the safety distance within the relevant range.

Based on data from a specific accident, it was found that simulating the possibility of a collision between a VRU and a drawbar trailer showed the pedestrian would not have been hit if the trailer had been equipped with an active turning assistant system. This analysis was performed using a simulation model specifically adapted for drawbar trailers. These findings support the recommendation to install active turning assistant systems not only on towing vehicles but also on drawbar trailers, in order to save lives and prevent serious injuries caused by collisions between towed trailers and VRUs. However, to ensure the

real-life applicability of this system and its simulation model for drawbar trailers, several key parameters must be precisely defined. A further, detailed parameter analysis will therefore be conducted and published as the next step in our research.

Author Contributions: Conceptualization, F.I., G.K., D.F. and I.L.; methodology, F.I.; software, A.M. and F.I.; validation, F.I.; formal analysis, F.I.; investigation, F.I. and G.K.; resources, F.I., G.K. and A.M.; data curation, F.I.; writing—original draft preparation, F.I.; writing—review and editing, F.I., D.F. and A.M.; visualization, F.I.; supervision, D.F. and I.L.; project administration, I.L. All authors have read and agreed to the published version of the manuscript.

Funding: The APC was funded by the Publications Support Program of Széchenyi István University (Győr, Hungary).

Institutional Review Board Statement: Not applicable.

Informed Consent Statement: Not applicable.

Data Availability Statement: The data presented in this study are available on request from the corresponding author due to privacy reasons.

Conflicts of Interest: Author Andreas Moser was employed by Dr. Steffan Datentechnik GmbH and Gyula Kőfalvi was employed by EBK-Hungary Kft. The remaining authors declare that the research was conducted in the absence of any commercial or financial relationships that could be construed as a potential conflict of interest.

Abbreviations

The following abbreviations are used in this manuscript:

VRU	Vulnerable Road User
ABS	Anti-lock Braking System
ACC	Adaptive Cruise Control
AEB	Advanced Emergency Braking
ADAS	Advanced Driver Assistance System
ASGA	Mercedes' Active Sideguard Assist
BA	Brake Assistant
EBA	Emergency Brake Assist
ESP	Electronic Stability Program
FEDR	Forensic Event Data Recorder
HGV	Heavy Goods Vehicle
LLM	Large Language Model
MBS	Multi-body System
TA	Turning Assistant
TCS	Traction Control System

References

1. DEKRA Automobil GmbH. *DEKRA Road Safety Report 2025 "The Changing Face of Mobility"*; DEKRA e.V. Corporate Communications: Stuttgart, Germany, 2025.
2. European Commission. *EU Road Safety Policy Framework 2021–2030—Next Steps Towards 'Vision Zero'*; European Commission: Luxembourg, 2020.
3. Chen, X.; Li, X.; Hou, Y.; Yang, W.; Dong, C.; Wang, H. Effect of eHMI-equipped automated vehicles on pedestrian crossing behavior and safety: A focus on blind spot scenarios. *Accid. Anal. Prev.* **2025**, *212*, 107915. [CrossRef] [PubMed]
4. Ostermaier, I.; Sandner, V.; Kolke, R. Vergleichstest von Nachrüstlösungen für Lkw zur Detektion von ungeschützten Verkehrsteilnehmern im toten Winkel. *Verkehrsunfall Und Fahrzeugtechnik (VKU)* **2019**, *57*, 210–219.
5. Michalke, T.; Niewels, F.; Lich, T.; Maurer, T. Driver assistance and sensors. In *Automotive Handbook*, 11th ed.; Dietsche, K.-H., Reif, K., Eds.; Robert Bosch GmbH, Business Division, Automotive Aftermarket: Karlsruhe, Germany, 2022; pp. 1804–1871; ISBN 978-1-119-91190-6.

6. Ballarin, C.; Reisgys, F.M.; Scherhaufer, I.; Tresp, C. Fahrerassistenzsysteme im Nutzfahrzeug. In *Handbuch Assistiertes und Automatisiertes Fahren*; Springer Vieweg: Wiesbaden, Germany, 2024; pp. 951–985; ISBN 978-3-658-38486-9.
7. Ignácz, F.; Bell, M. Presentation of Visibility Tests Performed from the Truck Driver Cabin; Development and Validation of Visibility Field Models. In Proceedings of the 19th EVU Congress Prague 2010, Prague, Czech Republic, 14–16 October 2010; Bradác, A., Semela, M., Vavra, L., Eds.; European Association for Accident Research and Analysis (EVU): Prague, Czech Republic, 2010; pp. 337–348.
8. Moser, A.; Steffan, H. New Sliding Tests and their Evaluation The ESP Simulation Model in PC-Crash. In Proceedings of the 17th EVU Conference, Nice, France, 6–8 November 2008; European Association for Accident Research and Analysis (EVU): Nice, France, 2008; pp. 233–241.
9. Moser, A.; Steffan, H. Simulation of active safety systems (ADAS) in PC-Crash. In Proceedings of the 24. EVU Conference, Edinburgh, UK, 15–17 October 2015; European Association for Accident Research and Accident Analysis (EVU): Edinburgh, UK, 2015; pp. 1–6.
10. Niewöhner, W. Braking—Steering Conflict of ADAS systems. In Proceedings of the EVU 25th Annual Congress, Bratislava, Slovakia, 20–22 October 2016; Kasanicky, G., Kolla, E., Macurová, L., Benecová, K., Eds.; EVU—European Association for Accident Research and Analysis: Bratislava, Slovakia, 2016; pp. 87–92.
11. Paula, D.; Böhm, K.; Kubjatko, T.; Schweiger, H.-G. Challenges in forensic reconstruction of traffic accidents involving Advanced Driver Assistance Systems (ADAS). In Proceedings of the 29th Annual Congress, Haifa, Israel, 6–7 October 2021; European Association for Accident Research and Analysis (EVU): Haifa, Israel, 2021; pp. 19–35.
12. Ritter, S.; Baur, A.; Müller, F. Simulation model for analysing the avoidability of turning accidents involving VRUs with the integration of available active safety systems. In Proceedings of the EVU 32nd Annual EVU Congress, Kufstein, Austria, 12–14 September 2024; European Association for Accident Research and Analysis (EVU): Kufstein, Austria, 2024; pp. 337–344.
13. König, T.; Paula, D.; Quaschner, S.; Schweiger, H.-G. Influence of Blind Spot Assistance Systems in Heavy Commercial Vehicles on Accident Reconstruction. *Sensors* **2024**, *24*, 1517. [CrossRef] [PubMed]
14. Kim, J.H.; Lee, J.H.; Choi, J.H.; Jeon, W.J. AEB Simulation Method Based on Vehicle Test Data for Accident Analysis of ADAS Vehicles. *Int. J. Automot. Technol.* **2024**, *25*, 261–277. [CrossRef]
15. Gulino, M.S.; Vichi, G.; Vangi, D. Validation of a virtual forward simulation tool for ADAS assessment. *Eur. Transp. Res. Rev.* **2025**, *17*, 25. [CrossRef]
16. Decker, T.; Kottig, J.; Meyer, M.-A. Software-defined Vehicle Accelerates Virtual Testing of ADAS-AD Functions. *ATZelectronics Worldw.* **2025**, *20*, 20–24. [CrossRef]
17. Gulino, M.S.; Vichi, G.; Cecchetto, F.; Di Lillo, L.; Vangi, D. A combined comfort and safety-based approach to assess the performance of advanced driver assistance functions. *Eur. Transp. Res. Rev.* **2025**, *17*, 6. [CrossRef]
18. Sinz, W.; Bernsteiner, S.; Hütter, B. En Route to the Virtual Verification of Automated Driving Functions. *ATZ Worldw.* **2023**, *125*, 44–47. [CrossRef]
19. Moser, A.; Steffan, H. Artificial Intelligence (AI) in Accident Reconstruction. In Proceedings of the 33rd Annual EVU Congress, Brasov, Romania, 25–27 September 2025; Page, Y., Wach, W., Dima, D., Bauder, M., Eds.; European Association for Accident Research and Analysis (EVU): Brasov, Romania, 2025; pp. 9–32.
20. Tudor, I.A.; Gîrbacia, F. The Use of Large Language Models in Road Accident Investigation. In Proceedings of the 33rd Annual EVU Congress, Brasov, Romania, 25–27 September 2025; Page, Y., Wach, W., Dima, D., Bauder, M., Eds.; European Association for Accident Research and Analysis (EVU): Brasov, Romania, 2025; pp. 33–46.
21. Bell, M.; Ignácz, F.; Kőfalvi, G. Analysis of truck crash tests (Examination of truck crashes around our practice). In Proceedings of the 20. EVU Annual Meeting of the EVU, Graz, Austria, 15–17 September 2011; European Association for Accident Research and Analysis (EVU): Graz, Austria, 2011; pp. 276–288.
22. Dr. Steffan Datentechnik Ges.m.b.H. PC-Crash, Software for the Simulation of Car Accidents. 2025. Available online: https://dsd.at/index.php?option=com_content&view=article&id=512:pc-crash-englisch-3&catid=37&lang=en&Itemid=159 (accessed on 8 July 2025).
23. Weyde, M.; Priester, J. Motorcycle Crash Tests at a High Speed Level against Standing and Moving Passenger Cars. In Proceedings of the 17th EVU Conference, Nice, France, 6–8 November 2008; European Association for Accident Research and Accident Analysis (EVU): Nice, France, 2008; pp. 125–142.
24. Kurzke, B.; Weyde, M. Optimization of multibody system for cyclists in PC-Crash. In Proceedings of the 26th Annual Congress of the European Association for Accident Research and Analysis, Haarlem, The Netherlands, 19–21 October 2017; European Association for Accident Research and Accident Analysis (EVU): Haarlem, The Netherlands, 2017; pp. 157–168.
25. Rose, N.A.; Carter, N. *An Analytical Review and Extension of Two Decades of Research Related to PC-Crash Simulation Software*; SAE Technical Paper 2018-01-0523; SAE International: Warrendale, PA, USA, 2018; pp. 1–18.

26. Urban, M.; Dauer, F.; Erbsmehl, C. Generating validating multibody simulation models of e-bikes for PC-Crash. In Proceedings of the 26th Annual Congress of the EVU, Haarlem, The Netherlands, 19–21 October 2017; European Association for Accident Research and Accident Analysis (EVU): Haarlem, The Netherlands, 2017; pp. 169–176.
27. Dr. Steffan Datentechnik. *PC-CRASH, A Simulation Program for Vehicle Accidents*; Dr. Steffan Datentechnik: Linz, Austria, 2025; pp. 1–772.
28. Wach, W. *Simulation of Vehicle Accidents Using PC-Crash*; Institute of Forensic Research Publishers: Cracow, Poland, 2011; pp. 1–616; ISBN 83-87425-68-0.
29. Fang, T.; Xu, F.; Zou, Z. Causal Factors in Elderly Pedestrian Traffic Injuries Based on Association Analysis. *Appl. Sci.* **2025**, *15*, 1170. [CrossRef]
30. Asadi, F. *Engineering Mathematics with MATLAB® and Simulink®*; Springer Nature: Cham, Switzerland, 2025; ISBN 978-3-031-85244-2. [CrossRef]

Disclaimer/Publisher's Note: The statements, opinions and data contained in all publications are solely those of the individual author(s) and contributor(s) and not of MDPI and/or the editor(s). MDPI and/or the editor(s) disclaim responsibility for any injury to people or property resulting from any ideas, methods, instructions or products referred to in the content.